Supplementary Information for

Pursuit of a high-capacity and long-life Mg-storage cathode by tailoring sandwich-structured MXenes@carbon nanospheres composites

Fanfan Liu,† Yongchang Liu,† Xudong Zhao, Xiaobin Liu, and Li-Zhen Fan*

Dr. F. F. Liu, Prof. Y. C. Liu, Dr. X. Zhao, Dr. X. Liu, Prof. L.-Z. Fan

Beijing Advanced Innovation Center for Materials Genome Engineering

Institute for Advanced Materials and Technology, University of Science and Technology Beijing, Beijing 100083, China

*E-mail: fanlizhen@ustb.edu.cn

†F. F. Liu and Y. C. Liu contributed equally to this work

Supplementary Figures and Tables

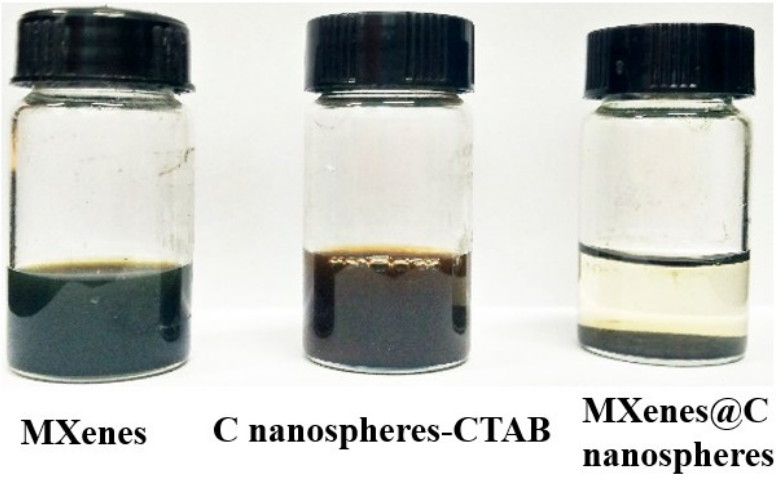

Fig. S1 Digital photographs of MXenes suspension, C nanospheres-CTAB in water, and MXenes@C nanospheres composites.

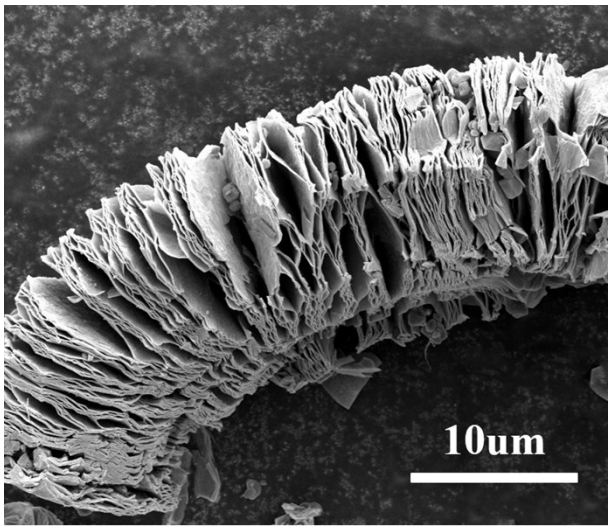

Fig. S2 Low magnification SEM image of the $Ti_3C_2T_x$.

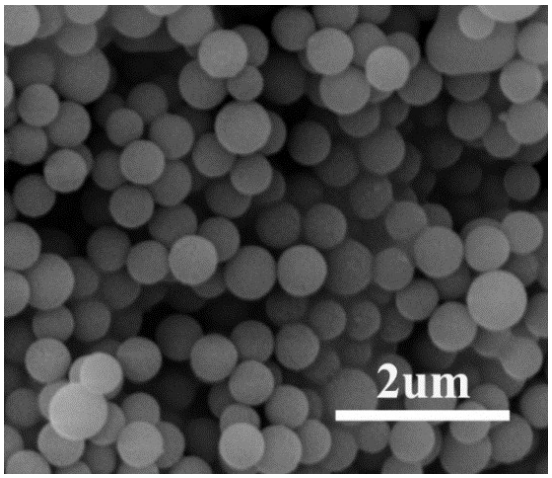

Fig. S3 SEM image of the carbon nanospheres.

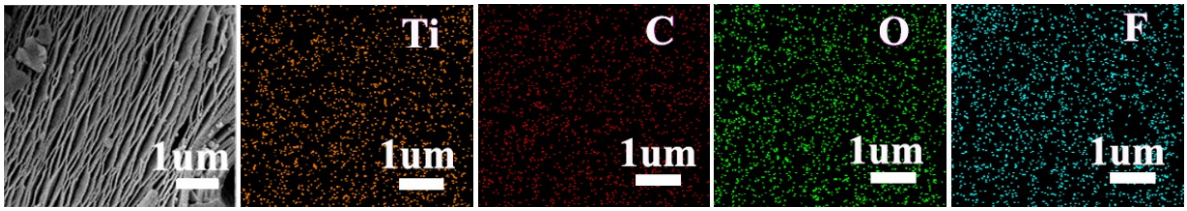

Fig. S4 EDS element mapping images of the $Ti_3C_2T_x$.

Table S1 Element contents (wt.%) of $Ti_3C_2T_x$ and $Ti_3C_2T_x$@C obtained from EDS.

Sample	Element (wt%)			
	Ti	C	O	F
$Ti_3C_2T_x$	56.9	19.4	17.6	6.1
$Ti_3C_2T_x$@C	49.94	29.6	15.89	4.57

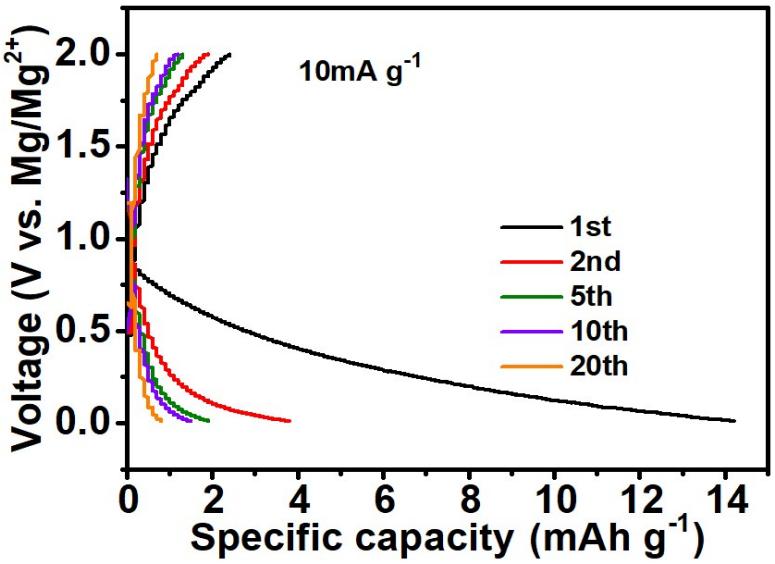

Fig. S5 Galvanostatic charge/discharge curves of the carbon nanospheres at 10 mA g^{-1}.

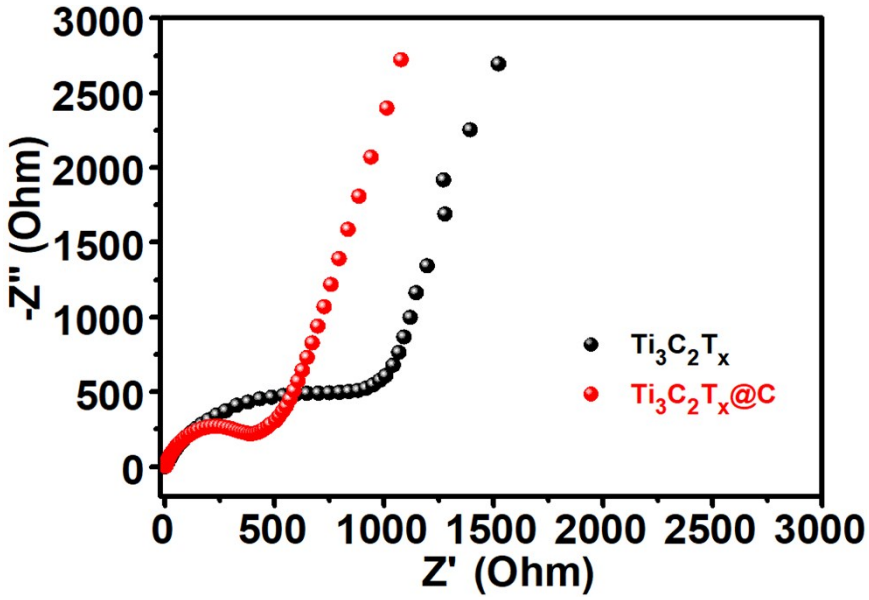

Fig. S6 Comparison of the EIS spectra of $Ti_3C_2T_x$ and $Ti_3C_2T_x$@C nanospheres electrodes.

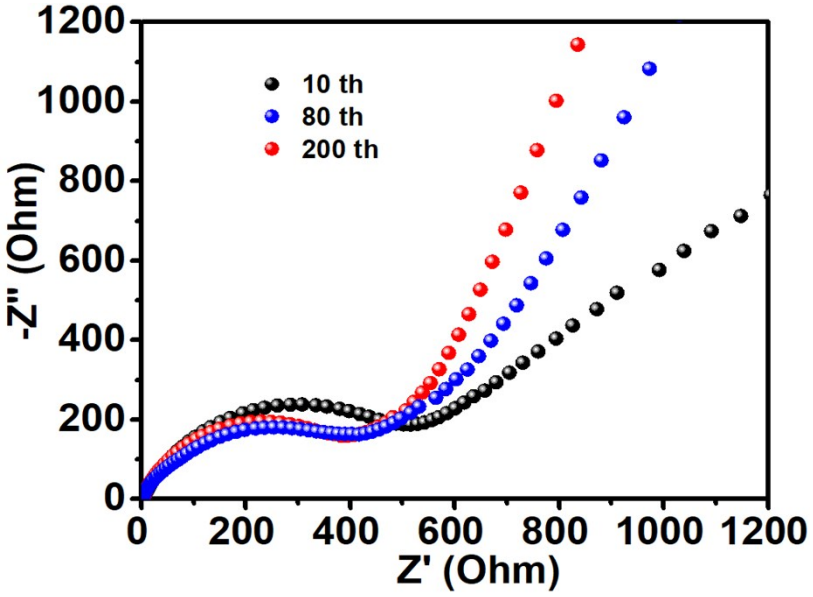

Fig. S7 EIS spectra of the $Ti_3C_2T_x$@C electrode after different cycles at 50 mA g^{-1}.

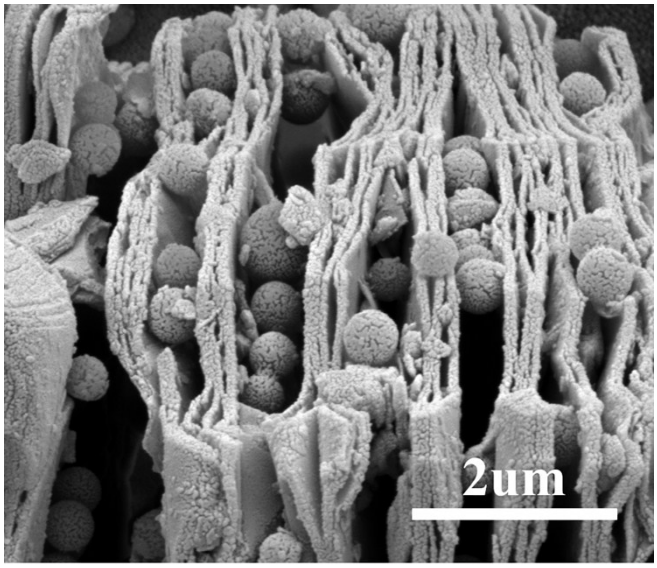

Fig. S8 SEM image of the $Ti_3C_2T_x$@C nanospheres after 400 cycles at 50 mA g^{-1}.

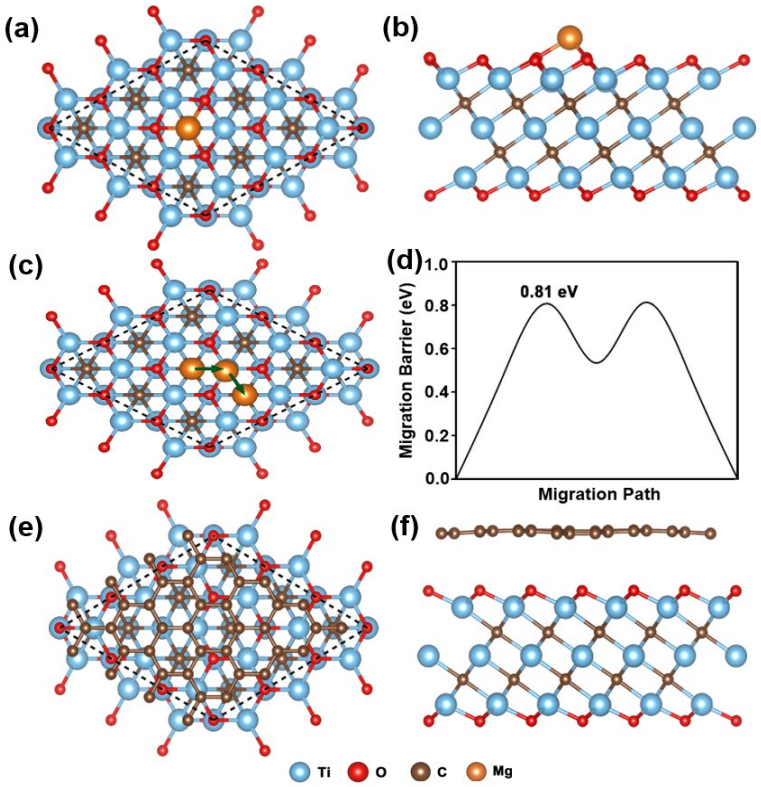

Fig. S9 (a, b) Top and side view of Mg ion adsorption on C sites of $Ti_3C_2O_2$, respectively. (c, d) The simulated migration path and diffusion profile of Mg ion on the $Ti_3C_2O_2$ surface, respectively. (e, f) Top and side view of the heterojunction model of $Ti_3C_2O_2$ and carbon layer, respectively.

Mg ion is preferentially adsorbed on the top site of C atom of $Ti_3C_2O_2$, at this site, Mg ion interacts with three O atoms on the surface, and it will be transported between two stable adsorption sites along the direction of the arrow. The intermediate state at the top site of Ti atom is another local stable adsorption position on the surface. And the migration barrier of magnesium ions is 0.81 eV, suggesting Mg^{2+} has a strong ability to adsorb on the $Ti_3C_2O_2$ surface. Thus, to simplify the calculation, in this study, we used a heterojunction model of $Ti_3C_2O_2$ and carbon layer to investigate the interaction between carbon spheres and $Ti_3C_2O_2$ in reality.

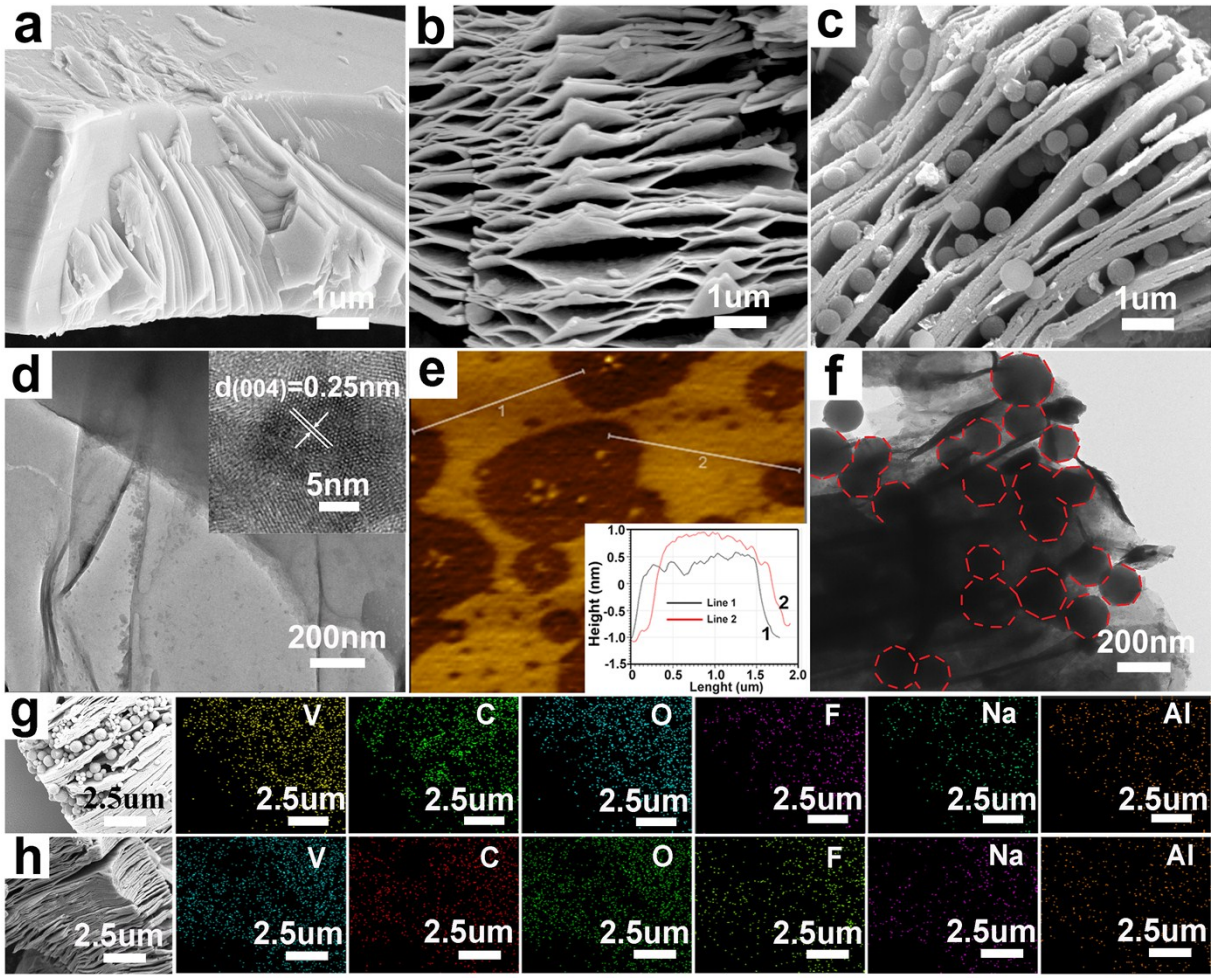

Fig. S10 SEM images of (a) V_2AlC, (b) V_2CT_x, and (c) V_2CT_x@C nanospheres. (d) TEM images of V_2CT_x, inset is HRTEM image of a typical V_2CT_x nanosheet. (e) AFM image and corresponding height profile of V_2CT_x nanosheets. (f) TEM image of V_2CT_x@C nanospheres. (g, h) EDS element mapping images of V_2CT_x@C nanospheres and V_2CT_x, respectively.

Similar to the $Ti_3C_2T_x$ MXene, after etching 72 h at 90 ºC, the densely layer-stacked structure of V_2AlC was exfoliated into accordion-like multilayer nanostructure of V_2CT_x MXene, and the sandwich-structured V_2CT_x@C nanospheres composites were obtained through electrostatic interaction between V_2CT_x and C nanospheres-CTAB. The V_2CT_x nanosheets are only few-

layers thick and the (004) lattice fringes spacing is measured to be 0.25 nm in the high-resolution TEM image. The thickness of V_2CT_x nanosheets can achieve as low as 1.5~2.1 nm, as estimated from direct measurements based on AFM image. TEM image of V_2CT_x@C nanospheres indicates that C nanospheres are inserted into the V_2CT_x layers, in great agreement with the SEM results. The EDS mapping images of V_2CT_x@C nanospheres and V_2CT_x nanosheets reveal the uniform distribution of V, C, O, F, Na, and Al elements. The corresponding element contents (wt.%) are listed in **Table S2**. The increased C content (9.22 wt.%) confirms that C nanospheres can be successfully embedded in V_2CT_x layers.

Table S2 Element contents (wt.%) of V_2CT_x and V_2CT_x@C obtained from EDS.

Sample	Element (wt%)					
	V	C	O	F	Na	Al
V_2CT_x	46.1	25.32	18.98	7.71	0.73	1.16
V_2CT_x@C	42.7	34.54	13.14	7.6	0.96	1.06

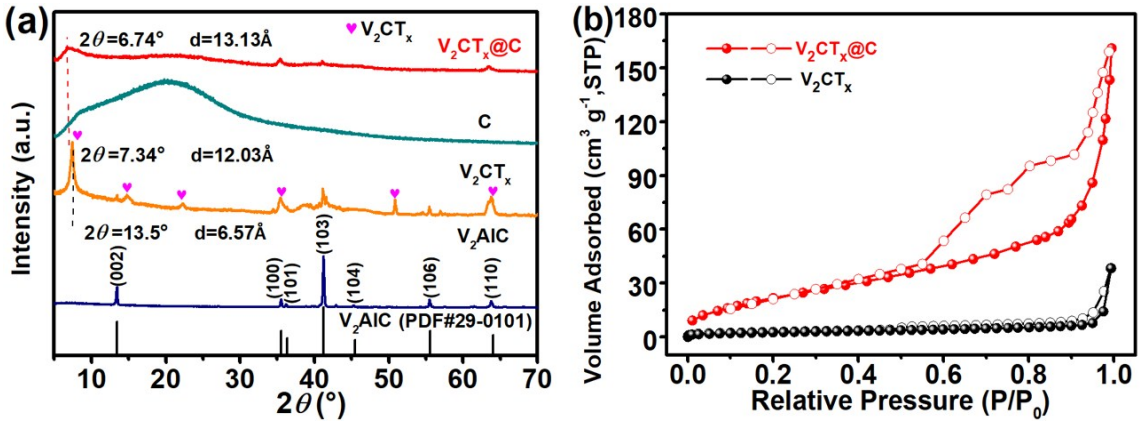

Fig. S11 (a) XRD patterns of the as-prepared samples. (b) N_2 adsorption-desorption isotherms of V_2CT_x@C nanospheres and V_2CT_x.

Compared with the peaks of the starting material V_2AlC, a new peak at 7.34º appears after etching 72 h at 90 ºC, and it belongs to V_2CT_x, this is consistent with the previous results.[1-3] However, weak peaks of V_2AlC still exist in the XRD patterns. After intercalation of C nanospheres, the (002) peak of V_2CT_x shifts from 7.34º to a lower angle of 6.74º, and the corresponding interlayer spacing increases from ~12.03 Å to ~13.13 Å. This provides considerable actives sites and rapid diffusion pathways for Mg^{2+} ions. Furthermore, the specific surface area of V_2CT_x@C nanospheres determined from N_2 adsorption/desorption isotherm analysis is increased to 96.3 $m^2\ g^{-1}$ compared with the pristine V_2CT_x MXene (10.6 $m^2\ g^{-1}$), this is beneficial for a high utilization rate of the active materials.

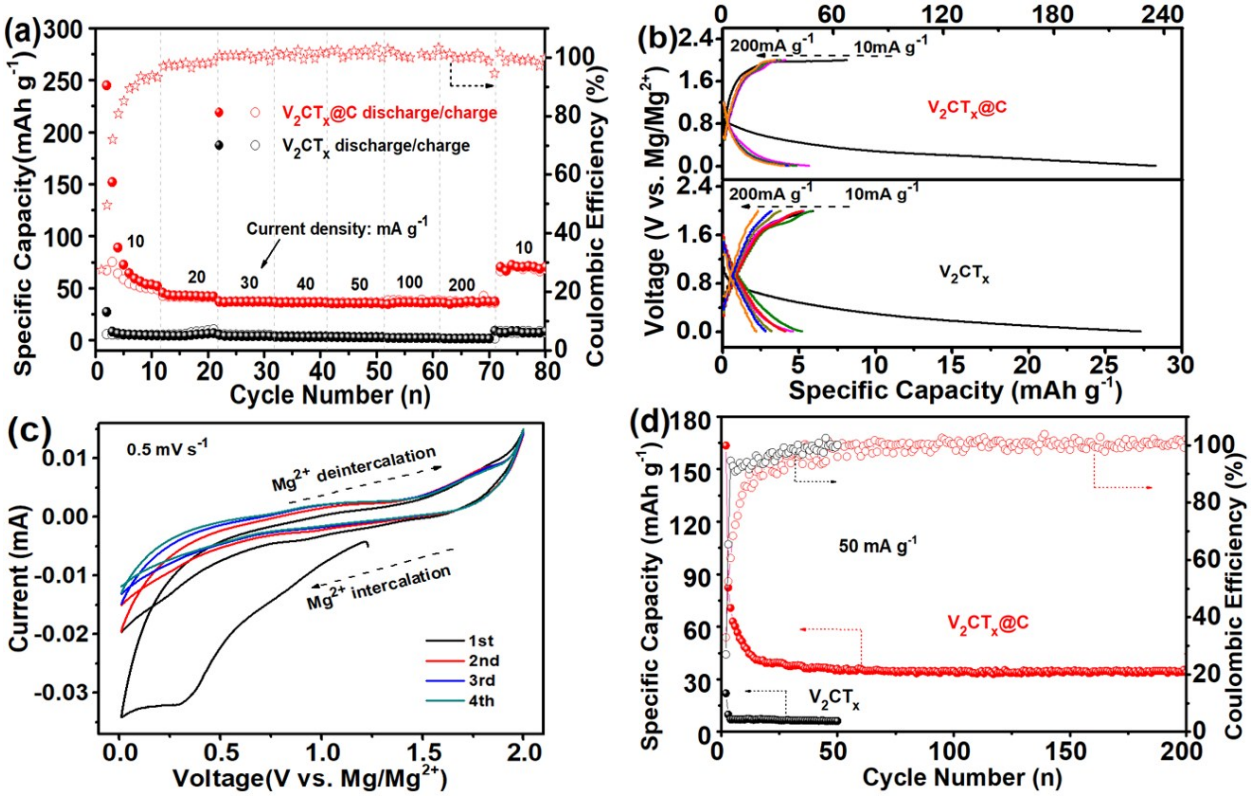

Fig. S12 (a) Rate capability of the V_2CT_x and V_2CT_x@C nanospheres electrodes, respectively. (b) Comparison of the galvanostatic charge and discharge curves under different current densities for V_2CT_x and V_2CT_x@C nanospheres electrodes. (c) CV curves of V_2CT_x@C nanospheres at a sweep rate of 0.5 mV s^{-1}. (d) Cycling performance of the V_2CT_x and V_2CT_x@C nanospheres electrodes at 50 mA g^{-1}.

Table S3 Comparison of the results in this work with those previously reported for the cathode materials of rechargeable Mg batteries.

Sample	Rate Capability	Cyclic Stability	Reference
C-Ti_2S_4	180 mA h g^{-1} at C/20 at 60℃ 175.5 mA h g^{-1} at C/10 at 60℃ 171 mA h g^{-1} at C/5 at 60℃ (1 C = 239 mA g^{-1})	~85% capacity retention at C/10 after 60 cycles	4
Graphene-like MoS_2	170 mA h g^{-1} at 20 mA g^{-1}	95% capacity retention at 20 mA g^{-1} after 50 cycles	5
Fluorinated Graphene Nanosheets (FGSs)	110 mA h g^{-1} at 10 mA g^{-1} 90 mA h g^{-1} at 50 mA g^{-1} 50 mA h g^{-1} at 100 mA g^{-1}	91% capacity retention at 10 mA g^{-1} after 30 cycles 89% capacity retention at 50 mA g^{-1} after 30 cycles 80% capacity retention at 100 mA g^{-1} after 30 cycles	6
TiS_2	160 mA h g^{-1} at C/20 140 mA h g^{-1} at C/10 90 mA h g^{-1} at C/5 (1 C = 239 mA g^{-1})	82.1% capacity retention at C/10 after 40 cycles	7
$Ni_{0.75}Fe_{0.25}Se_2$	190 mA h g^{-1} at 10 mA g^{-1} 120 mA h g^{-1} at 50 mA g^{-1}	98.2% capacity retention calculated from the 20th cycle at 20 mA g^{-1} after 50 cycles	8
CuS	165 mA h g^{-1} at 5 mA g^{-1} at 50℃ 117 mA h g^{-1} at 50 mA g^{-1} at 50℃	119 mA h g^{-1} at 50 mA g^{-1} after 30 cycles	9
MoS_2/rGO	104.2 mA h g^{-1} at 20 mA g^{-1} 87.5 mA h g^{-1} at 30 mA g^{-1} 80 mA h g^{-1} at 40 mA g^{-1} 76 mA h g^{-1} at 50 mA g^{-1}	74% capacity retention at 20 mA g^{-1} after 50 cycles	10
MoS_2/C microspheres	213 mA h g^{-1} at 50 mA g^{-1}	70% capacity retention at 50 mA g^{-1} after 50 cycles	11

CuFe-PBA	50 mA h g^{-1} at 0.1 A g^{-1} 45 mA h g^{-1} at 0.2 A g^{-1} 40 mA h g^{-1} at 0.5 A g^{-1} 37 mA h g^{-1} at 1 A g^{-1}	-	12
MoS_2/graphene	113.8 mA h g^{-1} at 20 mA g^{-1}	71% capacity retention at 20 mA g^{-1} after 50 cycles	13
Flower-like CoS	125 mA h g^{-1} at 50 mA g^{-1}	85% capacity retention at 50 mA g^{-1} after 60 cycles	14
$MgCoSiO_4$	167 mA h g^{-1} at 0.1 C 109 mA h g^{-1} at 0.2 C 86 mA h g^{-1} at 0.3 C 40 mA h g^{-1} at 0.6 C (1 C = 305.7 mA g^{-1})	~96.1 mA h g^{-1} at 0.2 C after 15 cycles	15
TiS_2 nanotubes	236 mA h g^{-1} at 10 mA g^{-1} 193 mA h g^{-1} at 20 mA g^{-1} 140 mA h g^{-1} at 40 mA g^{-1}	78% capacity retention at 0.2 A g^{-1} after 250 cycles	16
$Ti_3C_2T_x$/CTAB	100 mA h g^{-1} at 0.05 A g^{-1} 80 mA h g^{-1} at 0.1 A g^{-1} 67 mA h g^{-1} at 0.2 A g^{-1} 53 mA h g^{-1} at 0.5 A g^{-1} 42 mA h g^{-1} at 1 A g^{-1} 32 mA h g^{-1} at 2 A g^{-1}	67% capacity retention at 0.2 A g^{-1} after 250 cycles	17
MoS_2/$Ti_3C_2T_x$	165 mA h g^{-1} at 50 mA g^{-1} 140 mA h g^{-1} at 100 mA g^{-1} 93 mA h g^{-1} at 200 mA g^{-1} 53 mA h g^{-1} at 500 mA g^{-1}	65% capacity retention at 50 mA g^{-1} after 50 cycles	18
$Ti_3C_2T_x$@C nanospheres	198.7 mA h g^{-1} at 10 mA g^{-1} 183.8 mA h g^{-1} at 20 mA g^{-1} 154.8 mA h g^{-1} at 30 mA g^{-1} 147.9 mA h g^{-1} at 40 mA g^{-1} 144.6 mA h g^{-1} at 50 mA g^{-1} 137.1 mA h g^{-1} at 100 mA g^{-1} 123.3 mA h g^{-1} at 200 mA g^{-1}	85% capacity retention at 50 mA g^{-1} after 400 cycles	This work

Supplementary references

1. F. Liu, A. Zhou, J. Chen, J. Jia, W. Zhou, L. Wang and Q. Hu, *Appl. Surf. Sci.*, 2017, **416**, 781-789.
2. F. Liu, J. Zhou, S. Wang, B. Wang, C. Shen, L. Wang, Q. Hu, Q. Huang and A. Zhou, *J. Electrochem. Soc.*, 2017, **164**, A709-A713.
3. M. Naguib, J. Halim, J. Lu, K. M. Cook, L. Hultman,Y. Gogotsi and M. W. Barsoum, *J. Am. Chem. Soc.*, 2013, **135**, 15966-15969.
4. X. Sun, P. Bonnick, V. Duffort, M. Liu, Z. Rong, K. A. Persson, G. Ceder and L. F. Nazar, *Energy Environ. Sci.*, 2016, **9**, 2273-2277.
5. Y. Liang, R. Feng, S. Yang, H. Ma, J. Liang and J. Chen, *Adv. Mater.*, 2011, **23**, 640-643.
6. J. Xie, C. Lin, Z. Cui and X. Guo, *Adv. Funct. Mater.*, 2015, **25**, 6519-6526.
7. X. Sun, P. Bonnick and L. F. Nazar, *ACS Energy Lett.*, 2016, **1**, 297-301.
8. L. Zhou, F. Xiong, S. Tan, Q. An, Z. Wang, W. Yang, Y. Yao, Z. Tao, J. Chen and L. Mai, *Nano Energy*, 2018, **54**, 360-366.
9. F. Xiong, Y. Fan, S. Tan, L. Zhou, Y. Xu, C. Pei, Q. An and L. Mai, *Nano Energy*, 2018, **47**, 210-216.
10. Y. C. Liu, L. F. Jiao, Q. Wu, Y. Zhao, K. Cao, H. Liu, Y. Wang and H. Yuan, *Nanoscale*, 2013, **5**, 9562-9567.
11. Y. C. Liu, L. F. Jiao, Q. Wu, J. Du, Y. Zhao, Y. Si, Y. Wang and H. Yuan, *J. Mater. Chem. A*, 2013, **1**, 5822-5826.
12. Y. Mizuno, M. Okubo, E. Hosono, T. Kudo, K. Oh-ishi, A. Okazawa, N. Kojima, R. Kurono, S. Nishimura and A. Yamada, *J. Mater. Chem. A*, 2013, **1**, 13055-13059.

13. Y. C. Liu, L.-Z. Fan and L. F. Jiao, *J. Power Sources*, 2017, **340**, 104-110.

14. D. He, D. Wu, J. Gao, X. Wu, X. Zeng and W. Ding, *J. Power Sources*, 2015, **294**, 643-649.

15. Y. Zheng, Y. NuLi, Q. Chen, Y. Wang, J. Yang and J. Wang, *Electrochim. Acta*, 2012, **66**, 75-81.

16. Z.-L. Tao, L.-N. Xu, X.-L. Gou, J. Chen and H.-T. Yuan, *Chem. Commun.*, 2004, **18**, 2080-2081.

17. M. Xu, S. Lei, J. Qi, Q. Dou, L. Liu, Y. Lu, Q. Huang, S. Shi and X.-B. Yan, *ACS Nano*, 2018, **12**, 3733-3740.

18. M. Xu, N. Bai, H.-X. Li, C. Hu, J. Qi and X.-B. Yan, *Chin. Chem. Lett.*, 2018, **29**, 1313-1316.